JOURNAL OF MATERIALS SCIENCE **31** (1996) 3095–3107

# Mechanical properties of ethylene–α-olefin copolymers

J. G. FATOU, I. G. MACIÁ, C. MARCO, M. A. GÓMEZ
*Departamento de Física e Ingeniería de Polímeros, Instituto de Ciencia y Tecnología de Polímeros, C.S.I.C. Juan de la Cierva, 3. Madrid-28006, Spain*

J. M. ARRIBAS, A. FONTECHA, M. AROCA, M. C. MARTÍNEZ
*Repsol, S.A., Departamento de Investigación, Embajadores, 183. Madrid-28045, Spain*

The stress–strain behaviour at ambient temperature has been studied for a set of commercial polyethylenes. High density polyethylenes, HDPE, and linear low density polyethylenes, LLDPE, have been considered. In the first group, the linear structure is slightly modified by random copolymerization with the α-olefins, 1-propene, 1-butene and 1-hexene, at a concentration lower than 1% molar. In the second group, the comonomers employed were 1-propene, 1-butene, 1-hexene and 1-octene at a concentration lower than 3% molar. The structural variables, the level of crystallinity, the structure and amount of the interfacial and amorphous regions, and the size of the lamellar crystallites, have been correlated with the chemical structure of the ethylene–α-olefin copolymers and with the main characteristics of the deformation, the initial modulus, the yield stress and the ultimate properties, draw ratio and strength at break. The small deformation properties, modulus and yield, depend on the branch content but do not depend on the branch type. Consequently, these parameters were found to depend on the core crystallinity. On the other hand, the draw ratio at break was found to be invariant with the co-unit content and the core crystallinity. The ultimate tensile strength decreases when the mol % branch content increases. The final properties are found to depend on molecular weight.

## 1. Introduction

The mechanical behaviour of semicrystalline polymers is dominated by the viscoelastic characteristics of these systems. At very low deformation or at low deformation rates, the relationship between stress, strain and time are given by a series of constitutive linear equations. On the other hand, for finite and large deformations, these equations are more complex and the viscoelastic character is non-linear.

The stress–strain behaviour, obtained from deformation experiments and the ultimate properties, elongation and strength at break, are very important characteristics for semicrystalline polymers. However, the only mechanical process understood at the molecular level is the elastic deformation of rubber-like materials.

For semicrystalline materials, various theories have been introduced in order to understand the molecular deformation [1–6]. Many of these theoretical hypotheses have been recognized to be incorrect [7] although the importance of molecular weight and crystallinity have been considered [8–11].

One of the most extensively analysed polymers is polyethylene. Studies encompass linear polyethylenes [12–17] and branched and random ethylene copolymers [18–22]. Recently, the structural variables of polyethylenes have been exhaustively determined and have been correlated with mechanical behaviour.

Among the variables to be studied are the degree of crystallinity, the size of the lamellar crystallites and the crystallite thickness distribution, the structure and amount of the interfacial regions, the topology of the non-crystalline regions and the supermolecular structure or morphology. These variables are determined by the chemical structure, molecular weight and thermal history. These parameters have been correlated with the main characteristics of the generalized stress–strain curves, the initial modulus, the yield stress and the ultimate elongation and strength at break.

This type of analysis has been pioneered by Mandelkern and co-workers [23–28] for polyethylenes, and it has been shown to be a very good basis for the understanding of the mechanical properties. Such studies were first carried out on linear polyethylenes and random ethylene-1-alkane copolymers [23, 24], and later on mixtures of linear polyethylene and random ethylene copolymers [26]. In this case, the molecular weights in each series were matched in order to avoid complications due to differences in molecular weights and polydispersity.

More recently, an extensive study of linear polyethylenes has been focused on molecular weight fractions and polymers having the most probable molecular weight distributions, encompassing a wide molecular weight range [27]. Moreover, random

0022–2461

copolymers of ethylene with the most probable molecular weight and narrow composition distribution have been analysed [29].

In the present work, we have adopted the same methodology in order to study the mechanical properties of high density polyethylenes and linear low density polyethylenes. Our studies are concerned with commercial polymers in both sets of samples. In the first case, the chemical structure of ethylene is slightly modified by random copolymerization with α-olefins, and in the second case the nature of the α-olefin and the long and short branching of the polymer are changed.

Therefore, we extend the previous results on polyethylene [23–28] to a wider range of commercial polymers with different molecular weight distributions and with different α-olefin content, from almost linear polyethylenes to linear low density polyethylenes. The aim of this work is, in principle, to demonstrate the general validity of the previous conclusions on the correlation between the structural parameters of these polyolefins and the parameters describing the general stress–strain curves. These correlations are fundamental in order to describe or predict the mechanical properties of commerical polymers.

## 2. Experimental part

### 2.1. Materials

The polymers used in this study were wholly commercial polymers. The high density polyethylenes, HDPE, were obtained from different manufacturers and produced by different types of polymerization. Low pressure, Ziegler–Natta catalysed processes were used in some cases and Phillips catalysts were used for several other polymers. Copolymers in this group contain α-olefin co-units in concentrations lower than 1% molar. The comonomers were 1-propene, 1-butene, and 1-hexene. Twenty nine types were selected for this study, including polymers with different trade marks.

Linear low density polyethylenes were selected from different commercial manufacturers. In this group, 26 grades were selected containing the comonomers 1-propene, 1-butene, 1-hexene, and 1-octene at concentrations lower than 3% molar.

The type and concentration of branches was determined in all cases by $^{13}$C-NMR, by the usual methodology [30, 31], using a Brucker AC 300, 300 MHz, working at 75 MHz in trichlorobenzene at 100 °C. In a few cases, a higher temperature of 105 °C was used.

Viscosity molecular weight averages were obtained by intrinsic viscosity measurements using a modified Ubbelhode viscometer previously described [32, 33] in decalin solutions at 135 °C. The intrinsic viscosity–molecular weight relationship is given by [34]:

$$[\eta] = 6.77 \times 10^{-4} M_w^{0.67}$$

Moreover, the molecular weight characteristics for most of the samples were determined by gel permeation chromatography (GPC) by following conventional procedures. Weight and number average molecular weights were obtained with $M_w/M_n$ relations between 1.6 to 23.2 for the HDPE, and between 2.9 to 7.7 for LLDPE, respectively. The most relevant parameters for the polymers are summarized in Tables I and II.

TABLE I Characterization of HDPE

| | $M_w$ | $M_w/M_n$ | Comonomer | mol % |
|---|---|---|---|---|
| HDPE-1 | 83,300 | 5.4 | Propene | 0.21 |
| HDPE-2 | 310,900 | 23.2 | Butene | 0.1 |
| HDPE-3 | 371,700 | 1.6 | Butene | 0.12 |
| HDPE-4 | 134,700 | 6.4 | Butene | 0.23 |
| HDPE-5 | 226,100 | 4.6 | Butene | 0.23 |
| HDPE-6 | 175,200 | 5.5 | Butene | 0.4 |
| HDPE-7 | 317,600 | 21.8 | Butene | 0.48 |
| HDPE-8 | 272,800 | 15.6 | Butene | 0.59 |
| HDPE-9 | 246,800 | 8.5 | Hexene | 0.05 |
| HDPE-10 | 133,000 | 3.6 | Hexene | 0.05 |
| HDPE-11 | 224,900 | 9.2 | Hexene | 0.09 |
| HDPE-12 | 238,200 | 15.4 | Hexene | 0.1 |
| HDPE-13 | 72,200 | 4.2 | Hexene | 0.1 |
| HDPE-14 | 197,300 | 7.2 | Hexene | 0.11 |
| HDPE-15 | 341,900 | 9.6 | Hexene | 0.11 |
| HDPE-16 | 200,400 | 16.8 | Hexene | 0.15 |
| HDPE-17 | 135,300 | 7.2 | Hexene | 0.16 |
| HDPE-18 | 119,000 | 10.3 | Hexene | 0.16 |
| HDPE-19 | 60,300 | 3.9 | Hexene | 0.31 |
| HDPE-20 | 290,000* | – | Hexene | 0.46 |
| HDPE-21 | 236,000* | – | Hexene | 0.49 |
| HDPE-22 | 257,600 | 14.4 | Hexene | 0.52 |
| HDPE-23 | 206,100 | 8.1 | Hexene | 0.61 |
| HDPE-24 | 160,800 | 8.2 | Hexene | 0.78 |
| HDPE-25 | 213,200 | 10.3 | Hexene | 0.98 |
| HDPE-26 | 230,400 | 12.5 | Hexene | 1.08 |
| HDPE-27 | 81,300 | 6.9 | Propene/Hexene | 0.7 |
| HDPE-28 | 229,300 | 15.6 | Butene/Hexene | 0.16 |
| HDPE-29 | 173,800 | 15.5 | Butene/Hexene<br>4-methylpentene | 1.13 |

*$M_v$

TABLE II Characterization of LLDPE

| | $M_w$ | $M_w/M_n$ | Comonomer | mol % |
|---|---|---|---|---|
| LLDPE-1 | 75 100 | 4.5 | Propene | 1.75 |
| LLDPE-2 | 100 500 | 3.9 | Butene | 1.67 |
| LLDPE-3 | 87 700 | 4.0 | Butene | 1.83 |
| LLDPE-4 | 94 300 | 4.1 | Butene | 2.32 |
| LLDPE-5 | 51 900 | 3.2 | Butene | 2.46 |
| LLDPE-6 | 60 700 | 3.5 | Butene | 2.46 |
| LLDPE-7 | 10 800 | 3.9 | Butene | 2.57 |
| LLDPE-8 | 92 800 | 3.7 | Butene | 2.57 |
| LLDPE-9 | 47 900 | 2.9 | Butene | 2.57 |
| LLDPE-10 | 85 900 | 3.3 | Butene | 2.64 |
| LLDPE-11 | 50 400 | 3.6 | Butene | 2.66 |
| LLDPE-12 | 135 200 | 7.7 | Hexene | 0.6 |
| LLDPE-13 | 86 800 | 3.5 | Hexene | 0.92 |
| LLDPE-14 | 90 300 | 3.8 | Hexene | 1.41 |
| LLDPE-15 | 82 000 | 3.5 | Hexene | 1.45 |
| LLDPE-16 | 97 300 | 4.2 | Hexene | 1.81 |
| LLDPE-17 | 93 800 | 4.0 | Hexene | 1.9 |
| LLDPE-18 | 94 600 | 3.2 | Octene | 0.73 |
| LLDPE-19 | 90 700 | 4.0 | Octene | 0.84 |
| LLDPE-20 | 91 800 | 3.6 | Octene | 1.04 |
| LLDPE-21 | 90 300 | 3.4 | Octene | 1.06 |
| LLDPE-22 | 82 700 | 3.7 | Octene | 1.24 |

## 2.2. Techniques

Densities of the ethylene–α-olefin copolymers were determined in a Davenport density gradient column, consisting of a water–ethyl alcohol mixture, at a constant temperature of 23 °C. The degree of crystallinity, based on density, $(1\text{-}\lambda)_d$, was calculated by the method of Chiang and Flory [35], using 1.000 and 0.853 g cm$^{-3}$ for the densities at room temperature of the completely ordered and liquid-like regions, respectively.

Heats of fusion were measured in a Mettler TA 3000 differential scanning calorimeter, calibrated with indium. Between 5 to 10 mg of sample sealed in an aluminium pan over the temperature range from 0 to 160 °C was measured. The degree of crystallinity, $(1 - \lambda)_{\Delta H_0}$, was calculated from the ratio $\Delta H_a/\Delta H_u$, $\Delta H_a$ and $\Delta H_u$ being the apparent and the completely crystalline heats of fusion, respectively. For $\Delta H_u$, the value of 288.9 J g$^{-1}$ was used [36, 37].

The crystallinities were also determined by analysis of the wide angle X-ray diffractograms and from the Raman internal mode spectra. In the first case, the diffractograms were obtained using a Philips Geiger counter X-ray diffractometer with Ni-filtered $\mathrm{CuK}_\alpha$ radiation. Crystallinities were obtained by decomposing the scattering curve into the amorphous halo and the two crystalline reflections (1 1 0) and (2 0 0), determining the areas $F_a$ and $F_c$ of the two components [38]. Average crystallite sizes were also estimated from the integral widths of the (1 1 0) and (2 0 0) reflections, after subtraction of instrumental broadening, by use of the Scherrer equation.

Methods previously described [39, 40] were used in the Raman analysis. The spectra were obtained in a Jobin–Ybon Ramanor HG25 double monochromator. The 514.5 nm line of an Ar ion laser was used as the excitation source. From the internal mode region, the fraction of chain units in the perfect crystal, $\alpha_c$, the fraction of chain units in the disordered structure, $\alpha_a$ and the fraction comprising the anisotropic interfacial region, $\alpha_i$, are given by the following relations:

$$\alpha_c = I_{1416}/(I_T \times 0.46)$$

$$\alpha_a = I_{1080}/(I_T \times 0.79)$$

$$\alpha_i = 1 - \alpha_c - \alpha_a$$

In many cases, crystallite thickness, uncorrected for chain tilting, was determined from the analysis of the low frequency Raman longitudinal acoustic vibrational mode (LAM). The spectra were analysed according to the method previously described [41].

Although a crystallite size distribution can be obtained in all cases, only the crystallite thickness which corresponds to the maximum of the peak in the distribution has been considered here.

## 2.3. Mechanical properties

Tensile measurements were carried out on a Model 1122 Instron Dynamometer. Previously, specimens of each of the polymers were prepared by compression moulding, following a predetermined thermal history. Samples were kept in the press at 177 °C for 3 min, with an applied pressure of 1–2 kg cm$^{-2}$ for another 5 min and, finally, 200 kg cm$^{-2}$ for another 5 min, followed by controlled cooling at 15 °C min$^{-1}$. Dumbell-shaped speciment were cut out of the moulded sheets using a press operated die. The dimensions of the test specimens in the gauge region were: length, 25.4 mm, width, 6 mm and thickness, 1.7 mm, according to ASTM D638. These dimensions were measured to an accuracy of 0.02 mm.

All samples were drawn at ambient temperature, 23 °C, and the force–elongation curves were recorded at a draw rate of 50 mm min$^{-1}$. The initial modulus, $E$, is the stress divided by the strain at very low deformation levels. It was calculated from the initial part of the stress–strain curve, using a linear regression method. The yield stress, $Y$, is defined as the yield force divided by the initial cross-sectional area, and was taken to be the first maximum in the stress–strain curve. In those cases in which no definable maximum was observed, prior to rupture, the yield force was determined by the intersection of lines extrapolated from the Hookean region and the region after the inflection point, before the initiation of strain hardening. The ultimate tensile properties are the elongation and the tensile stress at break. The elongation or draw ratio after break, $\lambda_B$, is defined as the spacing of the fiducial marks after break, divided by their initial spacing. The tensile strength at break, UTS, was calculated by dividing the stress at rupture by the initial cross-sectional area. The true ultimate tensile stress, TUTS, is defined by the stress on the cross-section at break, and can be defined by UTS $\times \lambda_B$, if it is assumed that the deformation is uniform.

At least 10 curves were recorded for each sample and the deviations of the initial modulus, the yield strength and the elongation and the tensile strength at break, are of the order of $\pm 2.5\%$.

## 3. Results and discussion

### 3.1. Structural parameters

The characteristics of the samples examined in this work are summarized in Tables I and II. Most of the polymers have very low nominal co-unit contents between 0.05 to 2.6 mol %, and they are considered as linear or near linear polymers, corresponding to commercial HDPE grades from many different manufacturers. However, the branches associated with the copolymerization with these very low amounts of α-olefins are not incorporated into the crystal lattice to any significant extent in the solidification process. This fact has been previously shown when the size of the alkyl group is ethyl or higher alkyl terms [42]. However, methyl groups and small atoms such as chlorine may enter the lattice on an equilibrium basis [43, 44].

The crystallinity obtained by different methods varies from 46 to 78%, when density values are considered, and from 30 to 75%, when enthalpy measurements or Raman spectroscopic data were used. It is important to indicate that the values obtained by

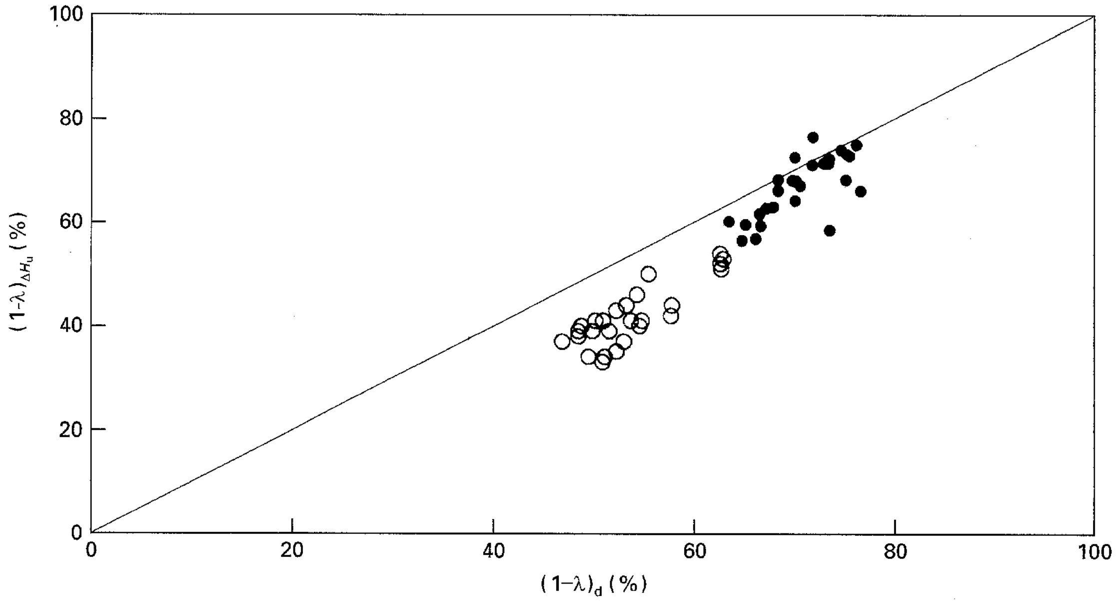

*Figure 1* Plot of core crystallinity from calorimetric measurements against crystallinity by density for: (●) HDPE; (○) LLDPE.

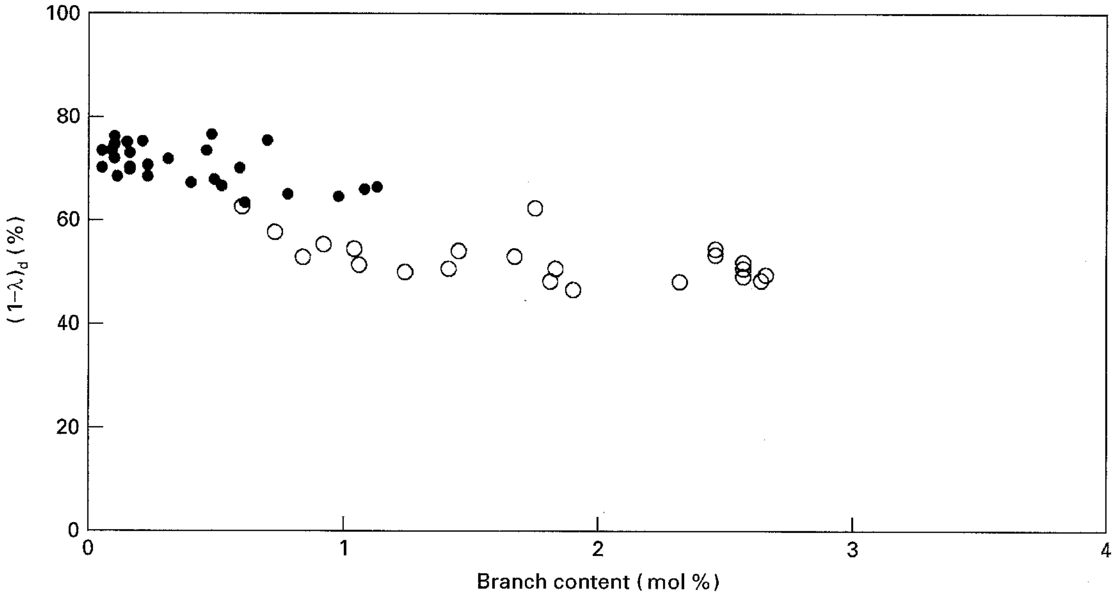

*Figure 2* Plot of crystallinity by density against branch content for random ethylene copolymers. (●) HDPE; (○) LLDPE.

density measurements are always higher than in the other two cases. As has been shown in previous works [44–46], this difference is related to the contribution of the interfacial region to the specific volume. The core crystallinity is related with $\Delta H_u$ or the Raman $\alpha_c$, defined above. The difference between $(1-\lambda)_d$ and $(1-\lambda)_{\Delta H_u}$ values is higher at lower crystallinity. The relation between both values in a very wide set of polymers, including samples with very high levels of crystallinity is illustrated in Fig. 1. It can be pointed out that, in spite of the different chemical structures of the co-units, the crystallinity values are independent of the structure and correspond solely to the co-unit content.

The trend of the curve shows very clearly that at the highest levels of crystallinity, in which the interfacial region is very small, the values of $(1-\lambda)_d$ tend to those of $(1-\lambda)_{\Delta H_u}$.

Moreover, the mole per cent of the branches dramatically influences the crystallinity in the polymers. Fig. 2 shows the decrease of $(1-\lambda)_d$ with the branch concentration. Again, it is important to point out that the experimental points correspond to polymers in which the co-units are different and, therefore, it can be concluded that the decrease in crystallinity with the concentration of branches is independent of the nature of the branch.

When the core crystallinity is measured, by Raman, $\alpha_c$, or by calorimetry, $[1-\lambda]_{\Delta H_u}$, the plot of crystallinity versus the co-unit content presents the same pattern as that of the density crystallinity, although crystallinity values are significantly lower, and the scattering of the experimental points is greater. Fig. 3 shows the plot of $(1-\lambda)_{\Delta H_u}$ versus the branch content. Finally, a new and interesting observation can be related to the differences in the behaviour shown by

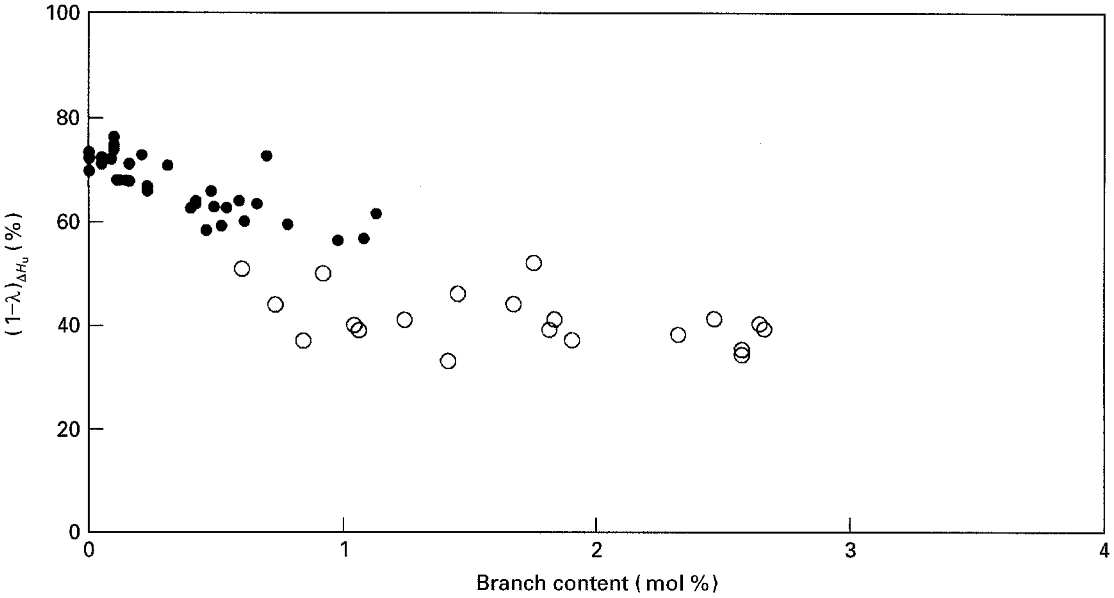

*Figure 3* Plot of core crystallinity from calorimetry against branch content for random ethylene copolymers. (●) HDPE; (○) LLDPE.

samples of copolymers with 1-butene. These show a decrease in crystallinity to lower values than those expected when the concentration of the branches increases. A possible explanation for this behaviour is the existence of differences in the distribution of the α-olefin co-units in the chain.

## 3.2. Tensile properties

In the discussion of the mechanical properties, the general characteristics of the stress–strain curve are considered, before examining the relationship between some of the mechanical parameters, such as the initial modulus and the yield stress, and the structural variables of the polymers. This is the same strategy adopted by Mandelkern and co-workers [23–28] in their fundamental and pioneering work on the mechanical properties of semicrystalline polymers.

It has been demonstrated [23, 27] that the structural variables have a very significant influence on the deformation process. Assuming a given chemical structure, the influence of molecular weight and the molecular weight distribution on the form of the stress–strain curve is very important. Very significant examples have been found in a variety of polyethylenes.

For homopolymers and for the lowest molecular weight samples, there is a well-defined yield where a necked region is established, a wide region where the force is invariant with the deformation and the neck propagates with a strain hardening phenomenon before failure.

At the other extreme, for the highest molecular weight samples, the yield region is barely perceptible, and the strain hardening dominates the deformation. Not only the molecular weight but also the molecular weight distribution of the samples plays an important role.

Thus, polyethylenes do not display a unique stress–strain curve and molecular and structural factors influence the character of the deformation process. Molecular weight and thermal treatment have a dramatic influence on the nature of the curves.

The brittle–ductile transition in linear polyethylene has been extensively studied [25, 27]. In principle, the parameter which controls the transition has been correlated with the draw ratio after break, $\lambda_B$. For $\lambda_B = 1$ the sample is brittle, and the sample is ductile when $\lambda_B$ is greater than unity. Therefore, $\lambda_B$ depends on the molecular weight and on the rate of deformation and a transition between the two types of deformation must exist.

Although the stress–strain curves will be considered in more detail below, in relation to the ultimate tensile properties, the partial variables of the deformation process, the initial modulus and the yield stress shall be analysed next.

## 3.3. Initial modulus

The first parameter of interest is the initial modulus, $E$, considered as the stress–strain ratio at infinitesimal deformation, calculated from the initial slope of the curve. The deformation which has been used in this work corresponds to 2%.

A plot of the moduli against the branch content is given in Fig. 4. There is a monotonic decrease in the modulus with increased branching. The modulus decreases from 1200 to 100 MPa in the range of branch contents from 0 to 2.7%. The higher dispersion in our data occurs at branch contents less than 1%. These values are consistent with those reported for other ethylene copolymers [23, 24]. Although the earlier studies demonstrated a complex behaviour and the plot of the modulus versus the density resulted in an S-shaped curve, further analysis has shown that the initial moduli for random ethylene copolymers can be approximated by a straight line which extrapolates very close to the origin.

The plot of the initial modulus against $(1-\lambda)_{\Delta H_u}$ in Fig. 5 has two regions, one up to 50% crystallinity in

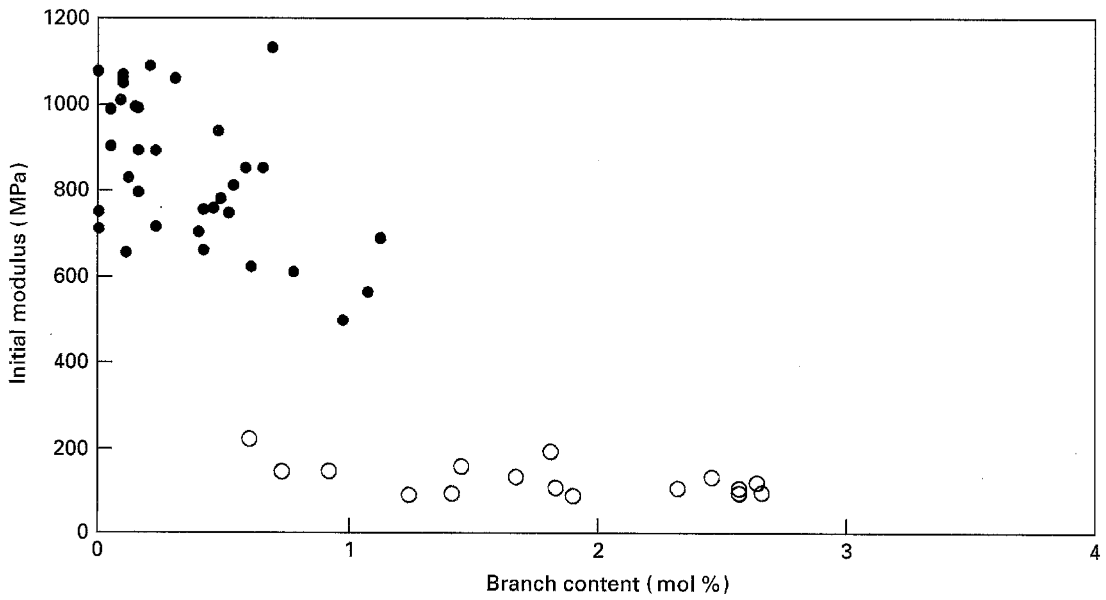

*Figure 4* Plot of initial modulus against branch content (mol %) for random ethylene copolymers. (●) HDPE; (○) LLDPE.

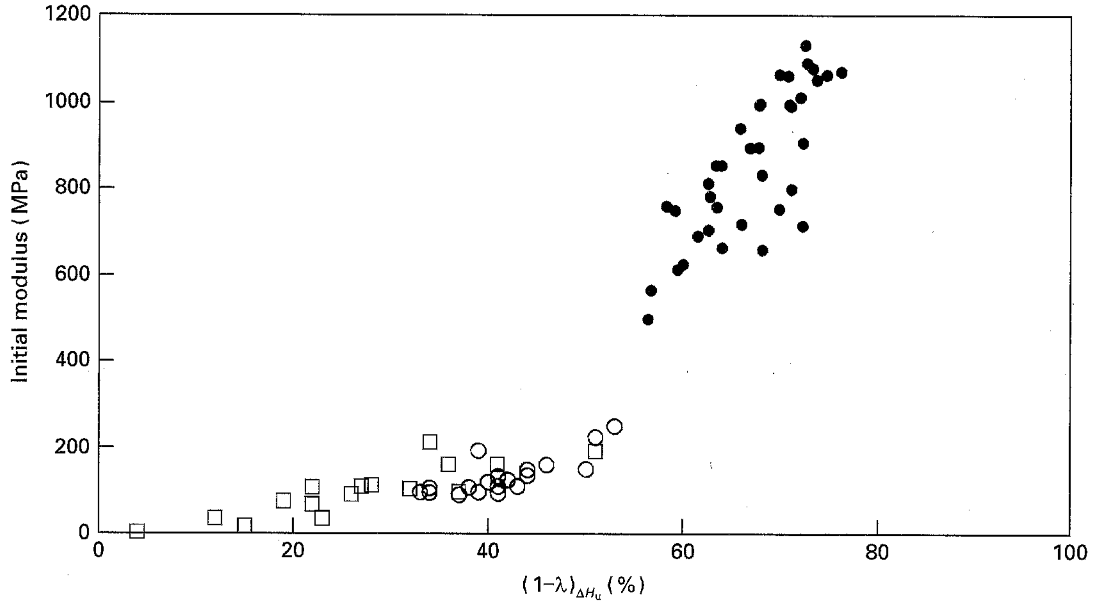

*Figure 5* Plot of initial modulus against core crystallinity by calorimetry for ethylene copolymers. (●) HDPE; (○) LLDPE; (□) some points from [23, 24].

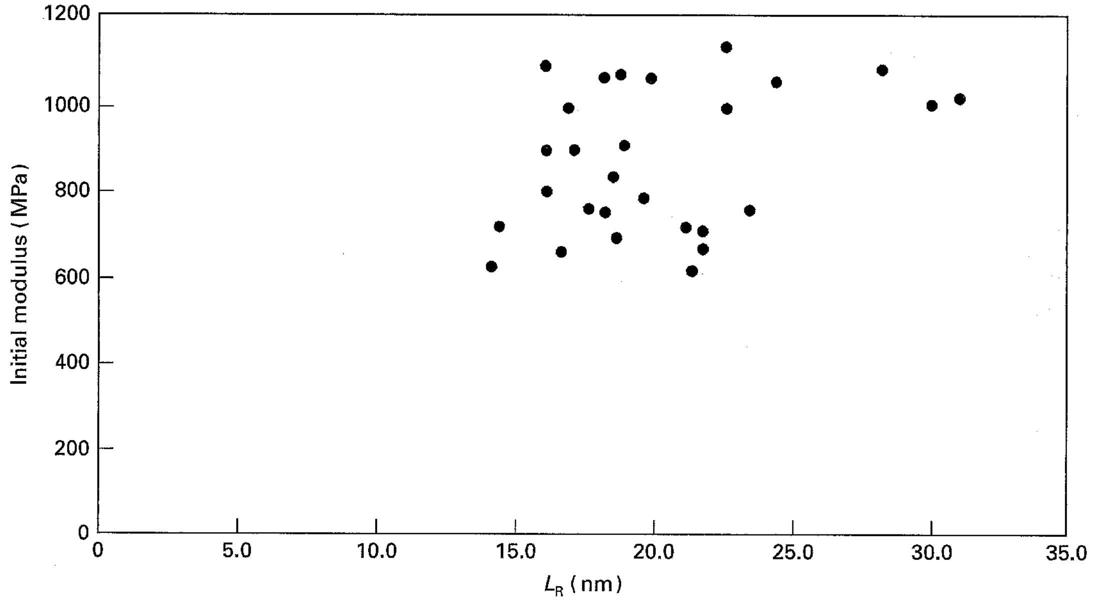

*Figure 6* Plot of initial modulus against crystalline size for HDPE.

which there is a linear relation and another from 60 to 80% in which the modulus is between three to five times higher than that found in the other region. For comparison of the curves and extrapolated lines some of the points from references [23] and [24] have been included in the low crystallinity range. The continuity of the results is evident.

The modulus does not depend on the supermolecular structure or the branch group in the copolymers with relatively small concentration of such groups. However, there is some correlation with both the crystallite size and the interlamellar zone. Fig. 6 shows the dependence of the modulus with the crystallite size as determined from the LAM in Raman spectroscopy. It has been shown [23] that the initial modulus decreases as a function of the interlamellar zone thickness. Therefore, the interfacial zone and the isotropic region play a very important role in the moduli of these systems. The crystallites seem to represent a high enhancement of the modulus compared with the case of a rubber–elastic polymer.

The reasons for the change of modulus with the phase structure have been discussed previously in great detail [23]. Several theoretical approaches have been considered [47–49] taking into account that the crystalline regions act as crosslinks or have a filler effect.

The classical models of Reus and Voigt have been applied to systems with very low and very high levels of crystallinity, respectively. Other approaches have used the combination of both models with adjustable parameters [50, 51]. Other explanations have been related to a composite model [52], which presents very good agreement between experiment and theory for high crystallinity values.

### 3.4. Yield stress

It is well established that the yield stress of polyethylene increases with the degree of crystallinity [23–28]. When the comparison is made against the degree of crystallinity calculated on the basis of density, the yield stress appears to be a linear function of the degree of crystallinity. When the corresponding degree of crystallinity, obtained from enthalpy measurements is plotted against the yield values, correlations are also clearly found. In Fig. 7 data reported in this work and some data points reported in the literature [22, 24] are plotted. The line is extrapolated to zero yield stress at 0–4% crystallinity.

It can be observed that the data reported in this work fall in the same region, although a shift is observed between the two types of data. This effect is probably due to different deformation rates, since it is well known that the yield stress increases with increasing strain rate. These results are also supported by the relation between yield and $\alpha_c$, in Fig. 8. Once again some data points reported previously [23, 24] are included and the continuity of the data is excellent in spite of the different origins of the samples. The extrapolation of this data to zero crystallinity suggests that a non-crystalline or very slightly crystalline sample does not display yield behaviour.

As has been previously considered, the relationship between the yield and the core crystallinity must have a corresponding relation between the yield and the branch content of the polymers. Fig. 9 shows this behaviour and, as expected, the lowest values of the yield correspond to the highest levels of branching, and hence correspond to the LLDPE samples.

On the other hand, a linear relationship which is extrapolated to zero yield and zero crystallite size has been found [23] between the yield stress and the maximum in the crystallite size distribution. However, in the present data, taking into account the dispersion of the values, the yield changes slightly with the crystallite size. With a crystallite size of between 15.0 to 31.0 nm the yield varies between 20 to 35 MPa, as shown in Fig. 10. These observations and the dispersion found experimentally may be a reflection of the crystallite distribution.

The molecular weight controls the crystallinity level which is attained, and thus, both parameters are interdependent. However, it has been pointed out recently [28] that at fixed crystallinity levels the yield becomes more diffuse when the molecular weight increases.

A correspondence between these two parameters is to be expected due to the fact that the initial moduli and the yield values present a correlation with the core crystallinity. The plot of yield stress ($Y$) versus initial modulus ($E$) is shown in Fig. 11. The yield seems to reach an asymptotic value at the highest values of the initial modulus.

In principle, the plastic deformation of semicrystalline polymers cannot be considered as the plastic deformation of low molecular weight materials in which the deformation is crystallographic in nature without changing the crystalline character.

Two different mechanisms have been suggested for yielding. Dislocation theories have been developed [53, 54] which predict the order of magnitude of the yield stress, but not its quantitative dependence on crystallite thickness. On the contrary, partial melting and recrystallization should occur when the temperature is raised or a stress is applied. A partial melting–recrystallization process has been postulated [55]. The fact that the yield stress decreases when the temperature increases, is attributed to a reduction in the energy requirements for partial melting. During deformation a heating process takes place and, when coupled with the applied stress, partial melting and recrystallization should occur [55–58]. Small angle neutron scattering studies support the melting and recrystallization process [59]. From other studies the same concept can be inferred [60–63].

None of the current hypotheses can predict the mechanism of the yielding and more experiments directed towards this goal are needed.

### 3.5. Ultimate tensile properties

The stress–strain curves of the different copolymers have been considered previously and it has been concluded that a universal curve for homopolymers and copolymers of ethylene does not exist. Linear polyethylenes can be ductile or brittle, depending on

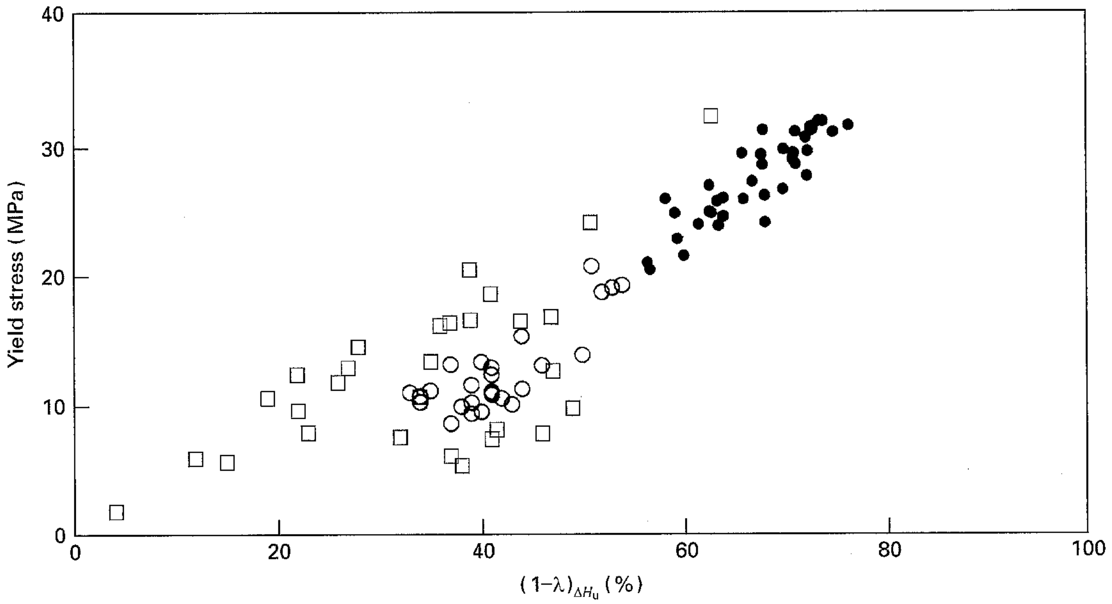

*Figure 7* Plot of yield stress against crystallinity from enthalpy measurements. (●) HDPE; (○) LLDPE; (□) experimental points from [23, 24].

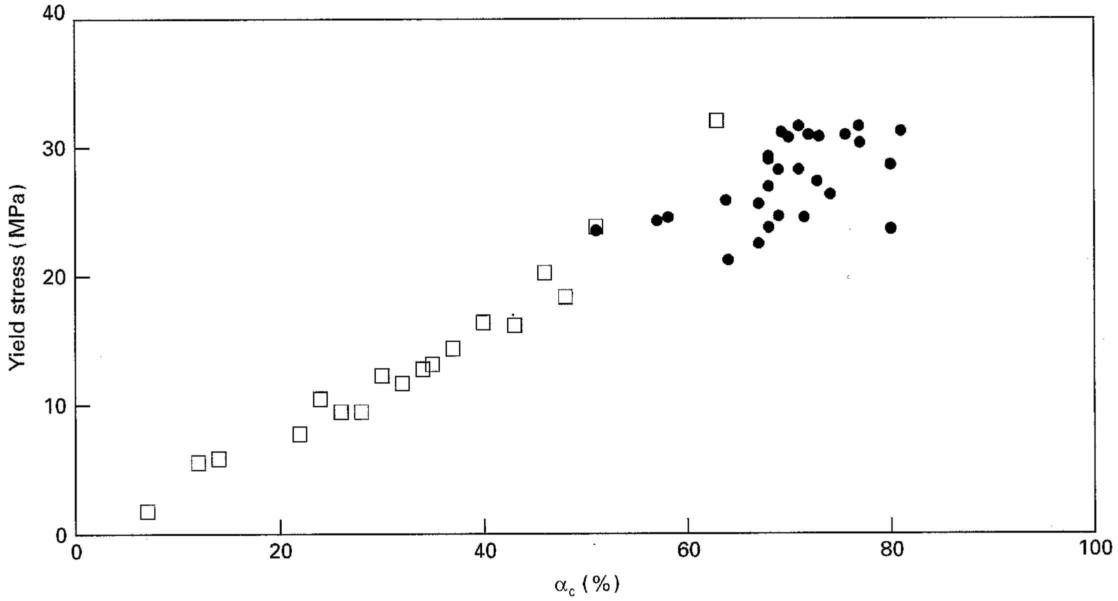

*Figure 8* Plot of yield stress against core crystallinity by Raman for ethylene copolymers. (●) HDPE; (□) selected points from [23, 24].

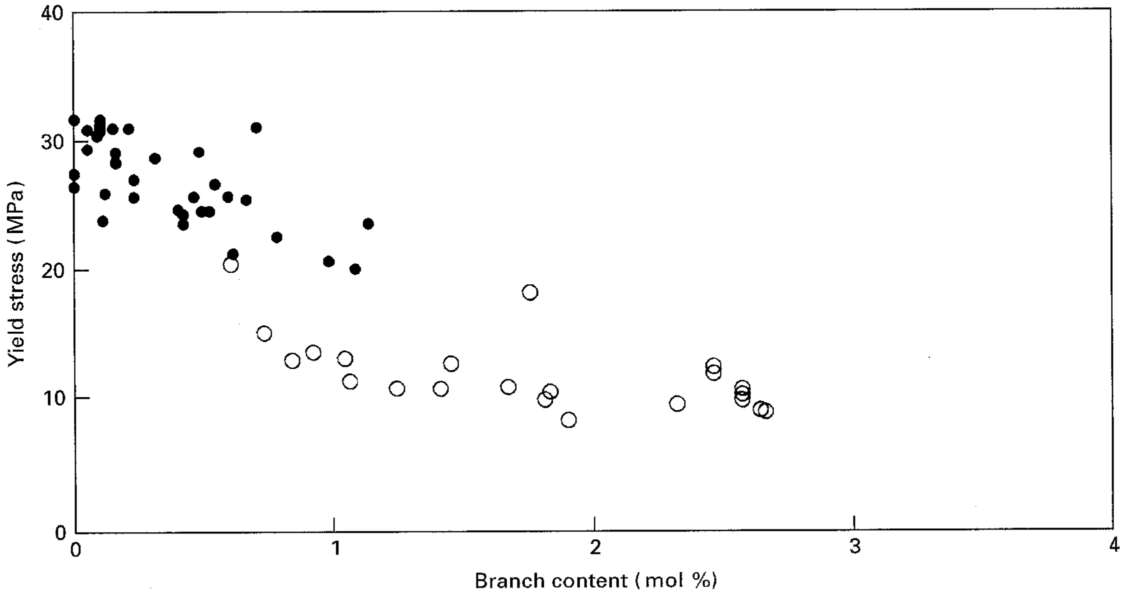

*Figure 9* Plot of yield stress against branch content (mol %). (●) HDPE; (○) LLDPE.

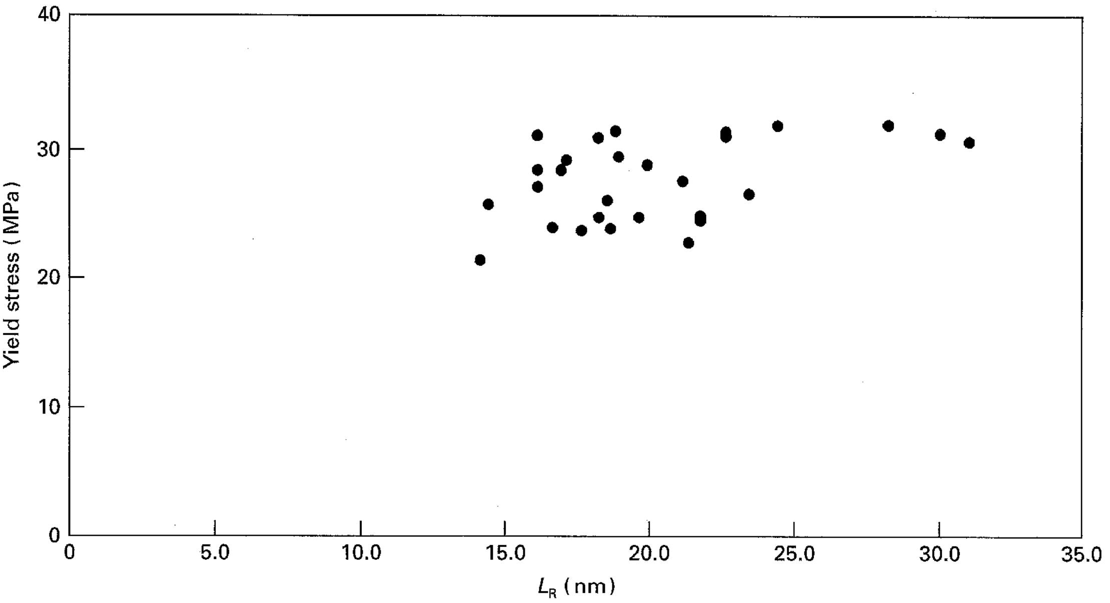

*Figure 10* Plot of yield stress against crystallite size for HDPE.

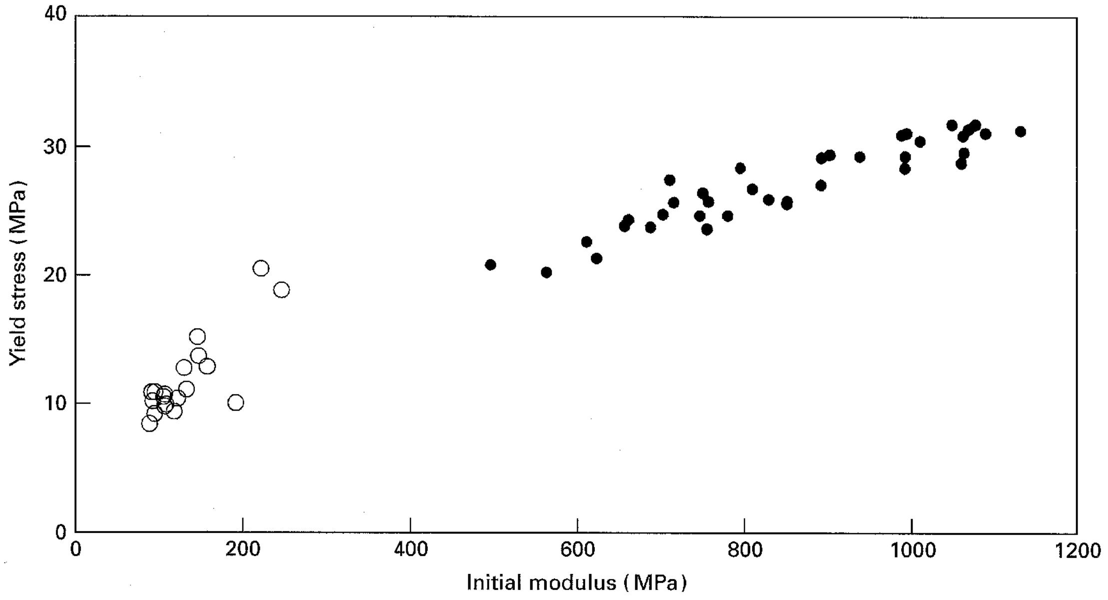

*Figure 11* Plot of yield stress against initial modulus. (●) HDPE; (○) LLDPE.

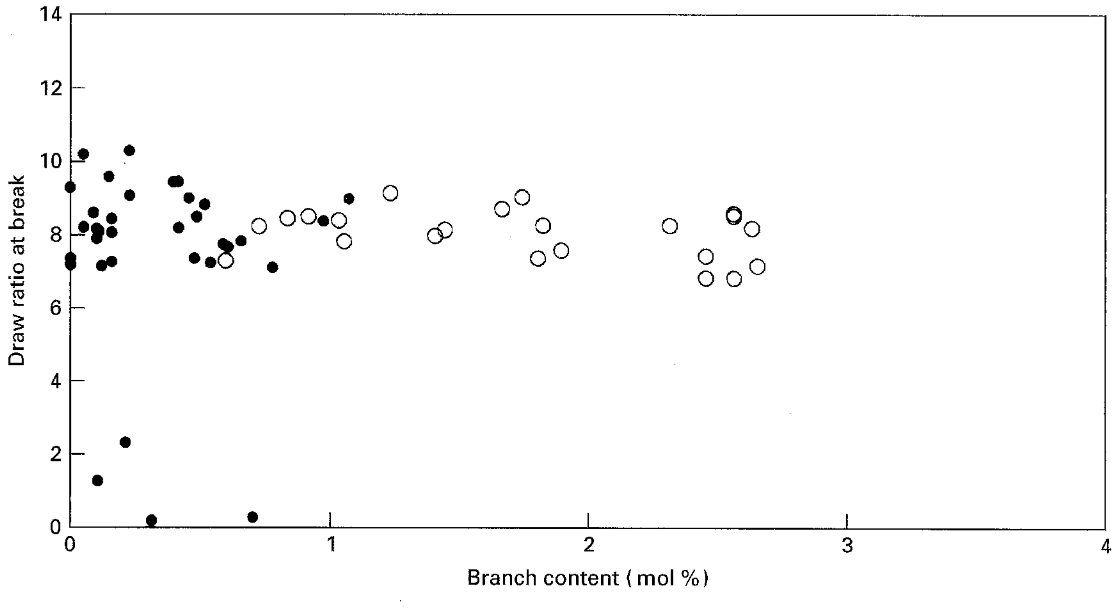

*Figure 12* Plot of draw ratio after break against branch content in the random ethylene copolymers. (●) HDPE; (○) LLDPE.

molecular weight, molecular weight distribution and thermal history or crystallization conditions, as previously discussed. However, in studying the deformation behaviour, certain general features should be analysed. Besides moduli and yield stress values which correspond to small deformation ranges, the elongation or draw ratio at break, $\lambda_B$, and the corresponding ultimate tensile strength, UTS or TUTS, are very important, practical parameters in the evaluation of the material. Therefore, these properties have been extensively studied in polyethylenes [9–11, 13]. Most of these studies have been carried out at elevated temperatures in order to obtain the largest draw ratio [9–13] and a conclusive influence of molecular weight on the draw ratio at break has been shown [13, 16, 64–66]. The most recent studies of ultimate tensile properties at room temperature are those of Mandelkern and coworkers [23–28], as previously indicated.

In order to analyse the importance of the structural parameters on the draw ratio at break, Fig. 12 shows a plot of this parameter versus the mole fraction of branches for all samples. It can be seen that $\lambda_B$ is practically invariant in the range from 6.5 to 10.0, irrespective of the type and concentration of the side groups, the molecular weight and molecular weight distribution. The only exceptions are the samples in which the draw ratio is below 4.0. These samples, HD-1, HD-13, HD-9 and HD-27, described in Table I, correspond to injection grades of commercial polymers. In these cases the molecular weights are comparatively low and the samples present a relatively narrow molecular weight distribution. In other

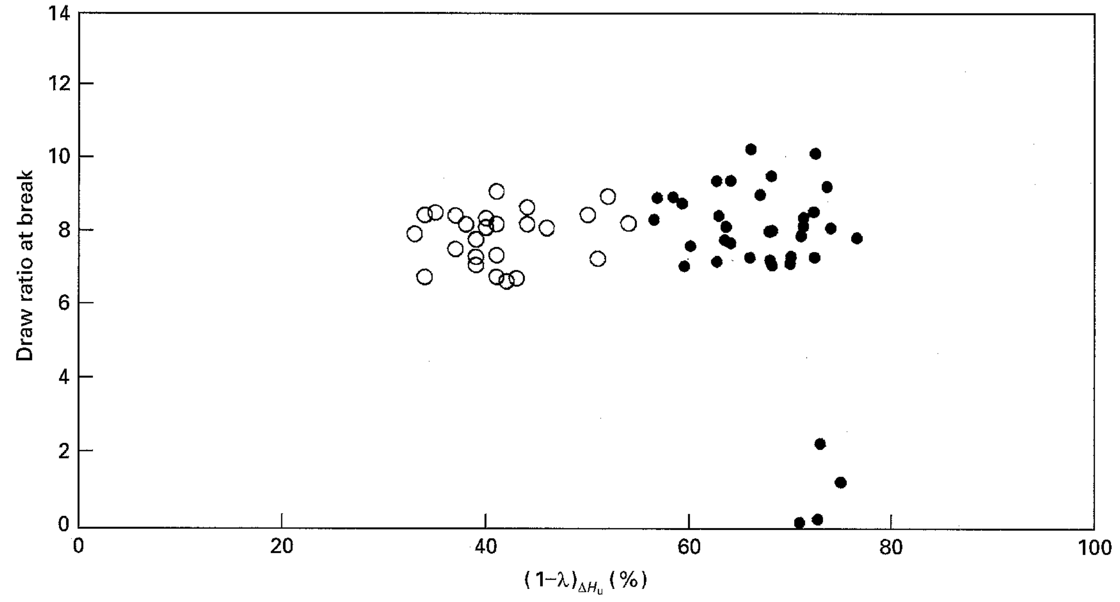

*Figure 13* Plot of draw ratio after break against crystallinity for calorimetric measurements. (●) HDPE; (○) LLDPE.

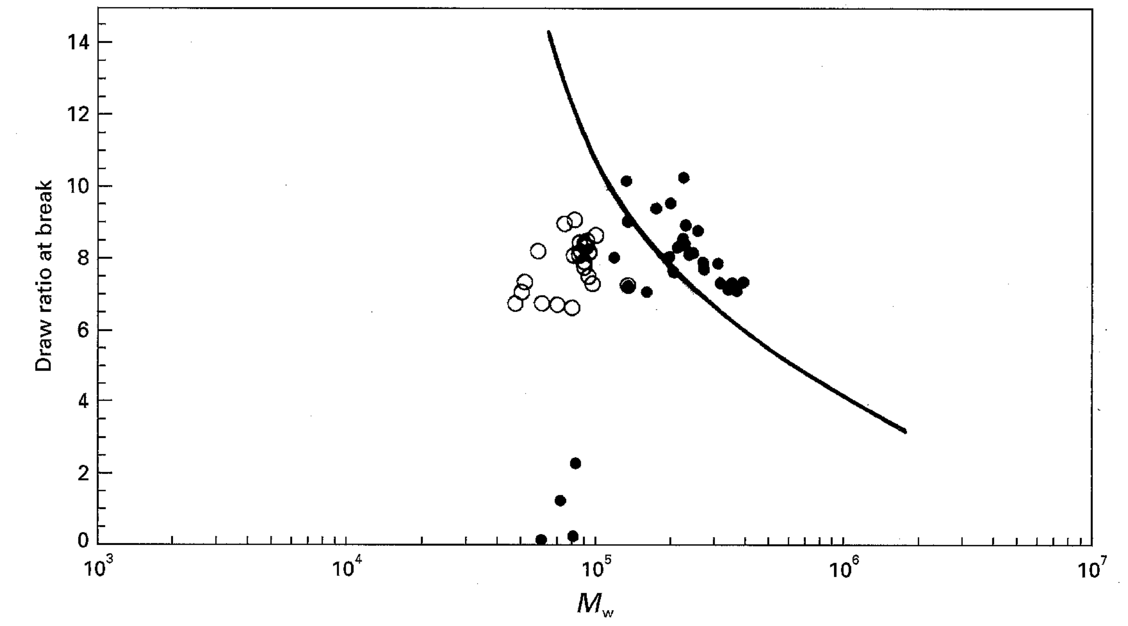

*Figure 14* Plot of draw ratio at break against weight-average molecular weight for random ethylene copolymers. (●) HDPE; (○) LLDPE; solid curve for unfractionated samples from [23].

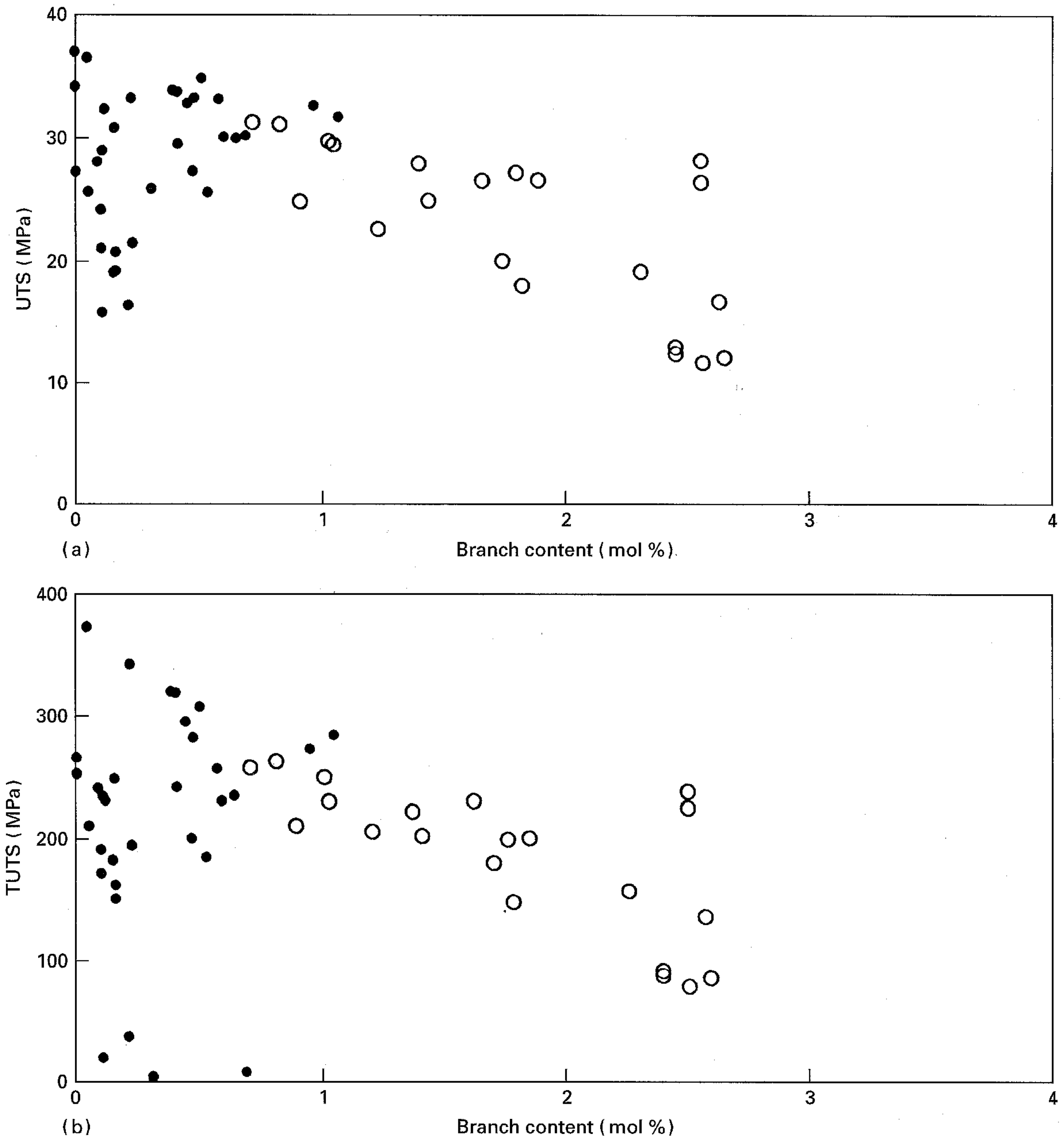

*Figure 15* Plot of the tensile strength against branch content in random ethylene copolymers. (a) Ultimate tensile stress, UTS; (b) true ultimate tensile stress, TUTS.

words, these samples are brittle or in the brittle–ductile transition region. Although the core crystallinity has been used to describe the type of deformation, other factors have been indicated as being the possible origin, including molecular weight and the structure of the interlamellar liquid-like region [27]. Both aspects are interlinked. At low molecular weights, there is not a sufficient amount of disordered chain segments connecting the crystallites and the thickness of the interlamellar region will be small. Therefore, the system cannot sustain large deformations.

As has been pointed out [23], one reason for the invariance in $\lambda_B$, shown in the region of 8.5 ± 1.50, even in the case of near-linear homopolymers, is the limited lateral extension of the crystallites of copolymers and of high molecular weight polyethylenes. It is well known that these crystallites present curved features and are highly segmented [67, 68].

The analysis of the core crystallinity or the density crystallinity of these polymers in relation with $\lambda_B$ leads to the same conclusions. In spite of the wide variations in the crystallinity in Fig. 13, from 35 to 75%, the elongation is once again 8.50 ± 1.50. The brittle polymers are those which do not follow the general behaviour and correspond to the injection grades with lower molecular weights.

Previous results on linear polyethylenes [23, 64] described the decrease in the draw ratio at break as a continuous curve with molecular weight, with a slight decrease in the slope of the curve at higher molecular weights. The plot of the draw ratio at break against molecular weight is given in Fig. 14, where our data for HDPE and LLDP are plotted together with the curve from [27]. Although a strong dependence of these two parameters has been reported, in our commercial polymer there are three types of data. Those which fit very well the general curve, HDPE, those with lower molecular weights and higher branching, LLDPE, which are more dispersed in relation with the curve, and finally, the brittle samples.

Although the range of molecular weights in the samples studied in this work is relatively narrow, the results are similar to those found in the analysis of polydisperse unfractionated polymers, fractions and polymers with most probable molecular weight distributions. It has been proposed that in branched polymers neither the molecular weight distribution nor the type and amount of branch groups affects the draw ratio. In other words, $\lambda_B$ is invariant irrespective of chemical structure and several features of the crystalline state, and it only depends on molecular weight.

On the other hand, the tensile strength at break, UTS, is related to the branch content, and decreases when the branching increases, Fig. 15a. Although there is a wide dispersion in the experimental points, this trend is clearly shown and this dependence for the ductile samples is more accentuated if the TUTS is considered, Fig. 15b.

When the core crystallinity increases a slight tendency to increase the value of the TUTS is observed.

The last parameter to be considered is the molecular weight. It has been established that the ultimate tensile stress for polyethylenes undergoing a ductile-type deformation depends only on its weight-average molecular weight. Plots of UTS and TUTS against molecular weight give a maximum at 100 000 and 30 000, respectively [27]. The results of our work are limited in molecular weights and, practically only a monotonic increase is observed in the plot of UTS, Fig. 16a, and an apparent maximum in the plot of TUTS, Fig. 16b.

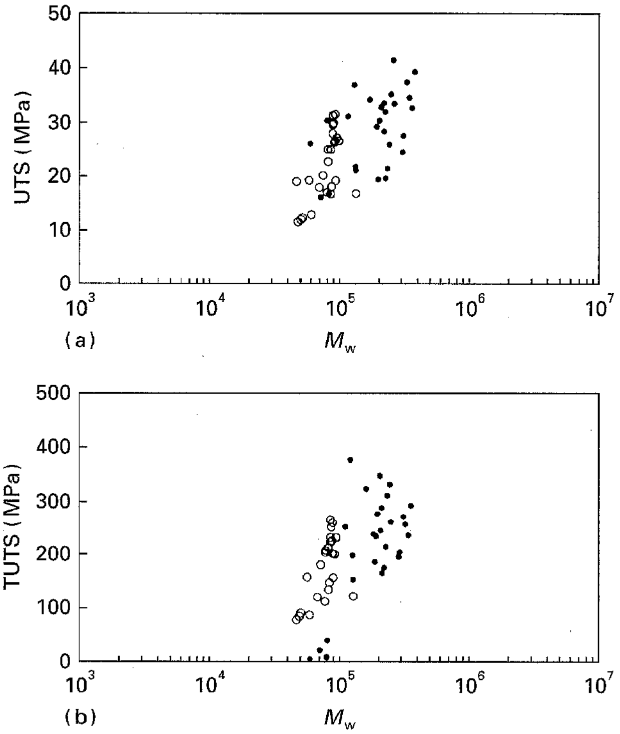

*Figure 16* Plot of the tensile strength against weight-average molecular weight. (a) Ultimate tensile stress, UTS; (b) true ultimate tensile stress, TUTS.

Therefore, one might expect that the deformation in the large strain region is correlated with the non-crystalline region. The response of the interlamellar region to the deformation has been experimentally [6, 55, 69–71] and theoretically studied [72, 73].

In conclusion, the ultimate tensile properties in the ductile region are a consequence of the topological features, entanglements, loops and interconnecting chain segments, which are located in the interlamellar region. These structures depend on the chain length, and, consequently, the dependence of the ultimate tensile properties on molecular weight can find an explanation in the elastic response of the interlamellar region.

## Acknowledgement

This work has been supported by a Cooperative Research Contract with Repsol. The authors are also grateful for the technical assistance of F. Prieto, A. Pérez, M. García and M. A. López.

## References

1. C. A. SPERATI, W. A. FRANTA and H. W. STARKWEATHER, *J. Amer. Chem. Soc.* **75** (1953) 6127.
2. A. PETERLIN, *J. Polym. Sci.* **C-9** (1965) 61.
3. R. HOSEMANN, *Polymer* **3** (1962) 349.
4. A. PETERLIN, *J. Polym. Sci.* **15** (1966) 427.
5. *Idem*, in "Man-Made Fibers", Vol. I, edited by H. F. Mark, S. M. Atlas and E. Cernia (Interscience, New York, 1967) p. 283.
6. S. ICHIARA and S. IIDA, in "The Strength and Stiffness of Polymers", edited by A. E. Zachariades and R. S. Porter (Dekker, New York, 1983) p. 129.
7. L. FISCHER, R. HASCHBERGER, A. ZIEGELDORF and W. RULAND, *J. Polym. Sci.* **260** (1982) 174.
8. G. CAPACCIO and I. M. WARD, *Polymer* **16** (1975) 239.
9. I. M. WARD, "Mechanical Properties of Solid Polymers", 2nd Edn (J. Wiley, New York, 1983).
10. J. STEIDL and Z. PELZBAUER, *J. Polym. Sci.* **38C** (1972) 345.
11. G. CAPACCIO, I. M. WARD and A. WILDING, *Discuss. Faraday Soc.* **68** (1979) 328.
12. A. PETERLIN, in "The Strength and Stiffness of Polymers", edited by A. E. Zachariades, R. S. Porter (Dekker, New York, 1983).
13. I. M. WARD, in "Ultra-High Modulus Polymers", edited by A. Ciferri and I. M. Ward (Applied Science, London, 1977).
14. N. BROWN and I. M. WARD, *J. Mater. Sci.* **18** (1983) 1405.
15. C. W. M. BASTIAANSEN, *J. Polym. Sci. Polym. Phys. Ed.* **28** (1990) 1475.
16. G. CAPACCIO and I. M. WARD, *ibid.* **22** (1984) 475.
17. R. W. IRUSS, P. L. CLARKE, R. A. DUCKETT and I. M. WARD, *ibid.* **22** (1984) 191.
18. K. SHIRAYANA, S. KITA and H. M. WATABE, *Makromol. Chem.* **151** (1972) 97.
19. W. PAYER, W. WICKE and B. CORNICH, *Angew. Makromol. Chem.* **94** (1981) 49.
20. A. TRAINOR, R. N. HAWARD and J. N. HAY, *J. Polym. Sci. Polym. Phys. Ed.* **15** (1978) 1077.
21. R. SEGUEDA and F. RIETSCH, *Polymer* **27** (1986) 703.
22. S. HOSODA and A. VERMURER, *Polym. J.* **24** (1992) 939.
23. R. POPLI and L. MANDELKERN, *J. Polym. Sci. Polym. Phys. Ed.* **25** (1987) 441.
24. A. J. PEACOCK and L. MANDELKERN, *ibid.* **28** (1990) 1917.
25. L. MANDELKERN, F. L. SMITH, M. D. FAILLA, M. A. KENNEDY and A. J. PEACOCK, *ibid.* **31** (1993) 491.

26. M. D. FAILLA and L. MANDELKERN, *Macromolecules* **26** (1993) 7167.
27. M. A. KENNEDY, A. J. PEACOCK and L. MANDELKERN, *ibid.* **27** (1994) 5297.
28. L. MANDELKERN, *A.C.S. Polymer Preprints* **36** (1995) 297.
29. M. A. KENNEDY, A. J. PEACOCK, M. D. FAILLA, J. C. LUCAS and L. MANDELKERN, *Macromolecules* **28** (1995) 1407.
30. J. C. RANDALL, *J. Polym. Sci. Polym. Phys. Ed.* **11** (1973) 275.
31. E. T. HSIEH and J. C. RANDALL, *Macromolecules* **155** (1982) 1402.
32. J. P. FLORY, A. C. CIFERRI and R. CHIANG, *J. Amer. Chem. Soc.* **83** (1961) 1023.
33. J. G. FATOU, "El Estado Cristalino en Polímeros" (Memoria del Premio Juan de la Cierva, Madrid, 1965).
34. P. S. FRANCIS, R. Jr. COOKE and J. H. ELLIOT, *J. Polym. Sci.* **31** (1957) 453.
35. R. CHIANG and P. J. FLORY, *J. Amer. Chem. Soc.* **83** (1961) 2057.
36. P. J. FLORY and A. VRIJ, *ibid.* **83** (1961) 2057.
37. L. MANDELKERN, J. G. FATOU, R. DENISON and J. JUSTIN, *J. Polym. Sci. Polym. Lett.* **3** (1965) 803.
38. H. HENDUS and G. SCHNELL, *Kunststoffe* **51** (1961) 69.
39. G. R. STROBL and W. HAGERDORN, *J. Polym. Sci. Polym. Phys. Ed.* **16** (1978) 1181.
40. G. R. STROBL and R. ECKEL, *ibid.* **14** (1976) 913.
41. R. G. SNYDER, S. J. KRAUSE and J. R. SCHERER, *ibid.* **16** (1978) 1593.
42. M. GLOTIN and L. MANDELKERN, *Colloid Polym. Sci.* **260** (1982) 182.
43. M. J. RICHARSON, P. J. FLORY and J. B. JACKSON, *Polymer* **4** (1963) 221.
44. M. KALEPKI, E. W. FISCHER, P. HERCHEURODER, J. SCHELLEN, G. LIESER and G. WEGNER, *J. Polym. Sci. Polym. Phys. Ed.* **17** (1979) 2117.
45. L. MANDELKERN, *Polymer J.* **17** (1985) 337.
46. *Idem*, in "Comprehensive Polymer Science" Vol. 2, Polymer Properties, edited by C. Booth and C. Price (Pergamon Press, New York, 1989).
47. S. NEWMAN, *J. Polym. Sci.* **47** (1960) 111.
48. L. E. NIELSEN and F. D. STOCKTONS, *ibid.* **A-1** (1963) 1945.
49. R. J. YOUNG, "Introduction to Polymers" (Chapman and Hall, London, 1981).
50. M. T. TAKAYANAGI, S. UEMURA and S. MINAME, *J. Polym. Sci.* **5C** (1964) 113.
51. M. TAKAYANAGUI, K. IMADA and T. KAJIYAMA, *ibid.* **15C** (1966) 263.
52. J. C. HALPIN and J. L. KARDOS, *J. Appl. Phys.* **43** (1972) 2235.
53. B. CRIST, C. J. FISHER and P. R. HOWARD, *Macromolecules* **22** (1989) 1709.
54. R. J. YOUNG, *J. Mater. Forum* **11** (1988) 210.
55. P. J. FLORY and D. Y. YOON, *Nature* **272** (1978) 226.
56. I. MARSHALL and A. B. THOMPSON, *Proc. R. Soc. London.* **221A** (1954) 221.
57. P. I. VINCENT, *Polymer* **1** (1960) 7.
58. D. C. HOOKWAY, *J. Textile Ind.* **49** (1958) 292.
59. G. D. WIGNALL and W. WU, *Polym. Commun.* **24** (1983) 354.
60. T. JUSKA and I. R. HARRISON, *Polym. Eng. Rev.* **2** (1982) 14.
61. T. SIN and I. R. HARRISON, *Polymer* **28** (1987) 1861.
62. A. N. GENT and J. JEONG, *J. Polym. Eng. Sci.* **26** (1986) 281.
63. A. N. GENT and S. MADAN, *J. Polym. Sci. Polym. Phys. Ed.* **27** (1989) 1529.
64. S. B. WARNER, *ibid.* **10** (1981) 1489.
65. H. YOSHIDA, K. TOMIZAWA and Y. KOBAYASHI, *J. Appl. Polym. Sci.* **24** (1979) 2777.
66. G. CAPACCIO, I. M. WARD and M. A. WILDING, *J. Polym. Sci. Polym. Phys. Ed.* **16** (1978) 2083.
67. I. G. VOIGT-MARTIN and L. MANDELKERN, *ibid.* **22** (1984) 1901.
68. I. G. VOIGT-MARTIN, R. ALAMO and L. MANDELKERN, *ibid.* **24** (1986) 1283.
69. G. CAPACCIO, J. A. CROMPTON and I. M. WARD, *ibid.* **18** (1976) 301.
70. P. SMITH, P. J. LEMSTRA and H. BOOIG, *ibid.* **17** (1981) 817.
71. L. FISCHER, R. HASCHBERGER, A. ZIEGELDORF and W. RULAND, *Colloid Polym. Sci.* **260** (1982) 174.
72. Y. TERMONIA and P. SMITH, *ibid.* **210** (1992) 1085.
73. Y. TERMONIA and P. SMITH, *Macromolecules* **21** (1988) 3485.

*Received 9 August*
*and accepted 21 December 1995*